Monte Carlo Simulation of Schottky Diodes Operating Under Terahertz Cyclostationary Conditions

P. Shiktorov, E. Starikov, V. Gružinskis, S. Pérez, T. González, L. Reggiani, L. Varani, and J. C. Vaissière

***Abstract*—We report Monte Carlo simulations of the current response and noise spectrum in heavily doped nanometric GaAs Schottky-barrier diodes (SBDs) operating under periodic large-signal conditions in the forward bias region. Due to the rather thin depletion region and heavy doping of these diodes, we find that the returning carrier resonance is shifted well above the terahertz region, so that the low-frequency noise plateau extends over the terahertz region. Here, frequency multiplication and mixing can take place at noise levels equal or below than that of full shot noise. We show that the signal-to-noise ratio of these SBDs is definitely superior to that of bulk semiconductors exploiting velocity-field nonlinearity.**

***Index Terms*—Cyclostationary operation, frequency multiplication, Monte Carlo (MC) simulation, Schottky barrier diodes, signal-to-noise ratio, terahertz generation.**

DUE TO THEIR strong nonlinear current–voltage (*I–V*) and capacitance–voltage (*C–V*) characteristics, GaAs Schottky-barrier diodes (SBDs) are widely used in modern solid-state electronics as frequency multipliers in the subterahertz region [1]–[3] and mixers in the superterahertz region [3]–[5]. As a consequence, the intensity of fundamental and higher order harmonics of the current response, the intrinsic noise, and the signal-to-noise ratio of these devices are relevant parameters when assessing their electrical performance under high-frequency large-signal operation. The aim of this work is to carry out a theoretical investigation of the above parameters in SBDs operating under periodic large-signal conditions in the terahertz frequency region typical of modern mixers and multipliers. For this sake, we consider the room temperature operation of a heavily doped GaAs n^+n-metal SBD with the same parameters of [5]: n region length $l_n = 0.03\ \mu$m, barrier height $U_b = 1.03$ V, carrier concentrations $n^+ = 8 \times 10^{18}$ cm^{-3} and $n = 1.1 \times 10^{18}$ cm^{-3}. The n^+ region length l_{n^+} has been reduced to 0.02 μm in order to optimize the computation time. The kinetic equation coupled with the Poisson equation for the self-consistent electric field is solved by the Monte Carlo (MC) method [6], [7]. $\Gamma - L - X$ nonparabolic spherically symmetric conduction band model and all main scattering mechanisms are accounted for in the MC simulations in accordance with [8]. The degeneracy effect is included by determining the final state after scattering with the rejection procedure of [9]. We are interested in large-signal operation near flat-band conditions, where Schottky diodes typically work. In this regime tunneling current plays a negligible role as compared to thermionic and displacement currents, and thus it is omitted. The self-consistent electric field is updated every 0.2 fs, with a total simulated history duration of about 3–10 ns and $N = 5$–10×10^3 particles. To compare the regular current response with the intrinsic noise level of the SBD under the same bias conditions, we implement a procedure recently developed for bulk semiconductors [10], [11]. Both the total current $J(t)$ and the spectral density of current fluctuations $S_{\delta J \delta J}(\nu)$ are normalized to the cross-sectional area A of the simulated SBD as $j(t) = J(t)/A$ and $s_{\delta J \delta J}(\nu) = S_{\delta J \delta J}(\nu)/A$, thus becoming quantities independent of A [7]

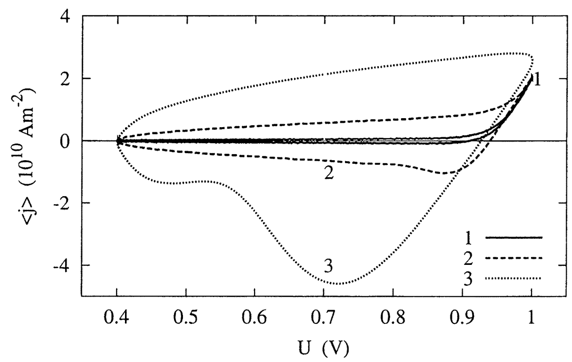

Fig. 1. Instantaneous total current density $\langle j \rangle$ as a function of the instantaneous periodic voltage $U(t) = U_0 + U_1 \sin(2\pi f t)$ applied to the SBD, with $U_0 = 0.7$ V, $U_1 = 0.3$ V and frequencies $f = 0.05$, 0.5, 2 THz (curves 1 to 3, respectively).

Fig. 1 reports the instantaneous total current density, $\langle j(t) \rangle$, flowing through the SBD as a function of instantaneous values of the applied voltage $U(t) = U_0 + U_1 \sin(2\pi f t)$ during a period of $U(t)$ oscillations for frequencies $f = 0.05$, 0.5, 2 THz (curves 1 to 3, respectively). Here brackets $\langle \cdots \rangle$ denote averaging over a large number of successive periods simulated by MC calculations. Values $U_0 = 0.7$ V and $U_1 = 0.3$ V are taken

Manuscript received September 9, 2003. This work was supported in part by the French-Lithuanian Bilateral Cooperation, the Italy-Spain Joint Action of the MIUR Italy, MCyT Spain, the Dirección General de Investigación (MCyT), FEDER through Grant TIC2001-1754, and the Consejería de Cultura de la JCyL through Grant SA057/02. The review of this letter was arranged by Editor T. Mizutani.

P. Shiktorov, E. Starikov, and V. Gružinskis are with the Semiconductor Physics Institute, 2600 Vilnius, Lithuania (e-mail: pavel@pav.pfi.lt).

S. Pérez and T. González are with the Departamento de Física Aplicada, Unversidad de Salamanca, 37008 Salamanca, Spain.

L. Reggiani is with the INFM—National Nanotechnology Laboratory, Dipartimento di Ingegneria dell' Innovazione, Università di Lecce, 73100 Lecce, Italy.

L. Varani and J. C. Vaissière are with the Centre d'Electronique et de Micro-optoelectronique de Montpellier, (CNRS UMR 5507) Universite Montpellier II, 34095 Montpellier Cedex 5, France.

Digital Object Identifier 10.1109/LED.2003.821635

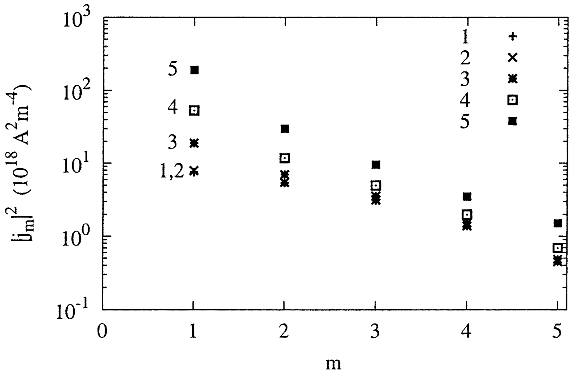

Fig. 2. Square amplitudes of the first five harmonics of the total current density as function of the harmonic order number m calculated for the same conditions of Fig. 1 at frequencies $f = 0.05$, 0.1, 0.5, 1, and 2 THz (symbols 1 to 5, respectively).

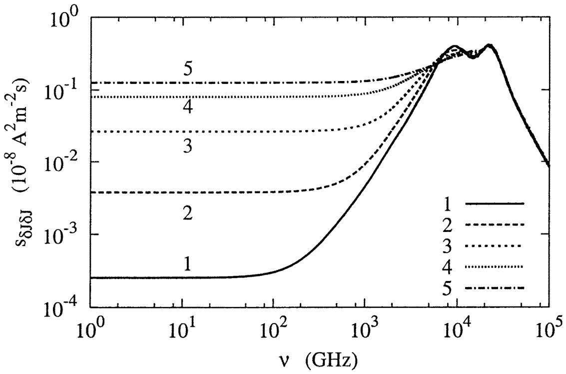

Fig. 3. Mean spectral density of current fluctuations calculated by the MC method for the n$^+$n SBD of Fig. 1 at $U_0 = 0.7$ V, $f = 2$ THz and $U_1 = 0.15$, 0.2, 0.25, 0.3, and 0.35 V (curves 1 to 5, respectively).

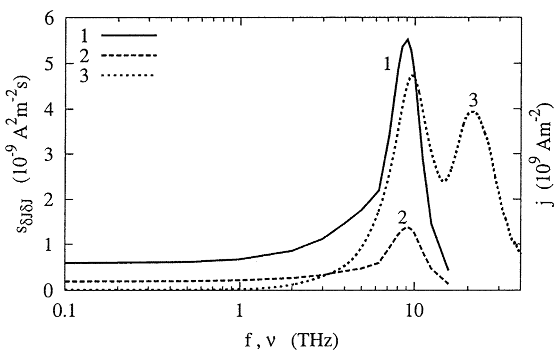

Fig. 4. Mean current density and low-frequency spectral density of current fluctuations as functions of the applied voltage frequency (curves 1 and 2, respectively). $U_0 = 0.7$ V, $U_1 = 0.25$ V. For comparison curve 3 shows the current noise spectrum under the static operation.

to exploit in the most effective way the nonlinear region of the *I–V* and *C–V* characteristics associated with the transition from barrier-limited to flatband conditions. This region corresponds to applied voltages comparable with the barrier height U_b. As follows from Fig. 1, the inertia of the current response is absent up to $f \approx 0.1$ THz. Here the $\langle j(U)\rangle$ diagram follows practically the static *I–V* relation. At $f > 0.1$ THz, the instantaneous $\langle j(U)\rangle$ characteristic begins to differ significantly from that of the static case. The hysteresis-like behavior of $\langle j(U)\rangle$ is accompanied by a rapid increase with f of the amplitude of both the fundamental and the higher order harmonics, what is typical for the strong *C–V* nonlinearity of varactor type [3]. This is illustrated by Fig. 2, which shows the squared amplitudes of the first five generated harmonics. For the SBD under test, the *C–V* nonlinearity dominates over the *I–V* nonlinearity in the frequency range 0.2–5 THz. At a further increase of f, the *C–V* nonlinearity becomes ineffective, since when approaching the returning carrier resonance [6] the displacement of the depletion region boundary no longer follows the instantaneous value of the applied voltage $U(t)$ (see also Fig. 4).

Under cyclostationary conditions, the current fluctuations $\delta J(t) = J(t) - \langle J(t)\rangle$ are described by the mean spectral density, $\overline{s}_{\delta J\delta J}(\nu)$, averaged over the period of oscillations. These spectral densities, calculated by using the correlation functions of current fluctuations [10], [11], are reported in Fig. 3 at fixed values $U_0 = 0.7$ V, $f = 2$ THz and increasing values of $U_1 = 0.15$, 0.2, 0.25, 0.3, and 0.35 V (curves 1 to 5, respectively). Here (and at lower frequencies f) the noise spectra of the SBD are found to exhibit the same features that these devices exhibit when operating under static voltage conditions [6]. Indeed, there always exists a low-frequency plateau, which is analogous to that of shot noise in the static case. However, in this case the plateau value strongly increases with U_1. Then, the spectra exhibit two peaks before decaying at the highest frequencies. The first peak around 10 THz is related to the so called returning carriers, electrons that after reflection from the barrier return to the emitting region. The second peak around 20 THz is associated with the spontaneous plasma oscillations and is typical of n^+n homojunctions [7].

Fig. 4 reports the low-frequency noise and the mean current density, $\overline{s}_{\delta J\delta J}(0)$ and $\overline{j}$, respectively, as functions of the frequency f of the applied voltage. For comparison, curve 3 shows the noise spectrum $\overline{s}_{\delta J\delta J}(\nu)$ calculated at $U_1 = 0$, i.e., under static operation. As follows from Fig. 4, $\overline{s}_{\delta J\delta J}(0)$ and $\overline{j}$ are practically independent of f up to values of f comparable with the returning carrier frequency [12] where both quantities exhibit a resonant enhancement.

For a fixed value of U_0, the increase of the low-frequency noise with U_1 is expected to follow that of the average current in accordance with the $2q\overline{J}$-law. To confirm this expectation, the low-frequency value $\overline{s}_{\delta J\delta J}(0)$, calculated at different frequencies f and amplitudes U_1, is reported in Fig. 5 as function of the mean current density for $U_0 = 0.7$ V. Here, at $U_1 \le 0.25$ V the full shot-noise law is confirmed for all frequencies. At $U_1 \ge 0.3$ V, results show a suppression of the low-frequency noise with respect to the full shot-noise law. The effect is more pronounced the greater U_1. Such a behavior is caused by the transition from barrier-limited transport (exponential part of static *I–V* relation) to flatband conditions (linear and saturation regions of the *I–V* relation), which occurs when the maximum value of the applied voltage $U_0 + U_1$ becomes greater than the barrier height U_b[6]. As follows from Figs. 4 and 5, the shot-noise suppression starts depending on frequency at $f \approx 10$ THz, i.e., near the returning carrier resonance. With a further increase of f, the shot-noise suppression is found to sharply disappear, thus recovering the $2q\overline{J}$ law. This is caused mainly by the reduction of the influence of the ac voltage com-

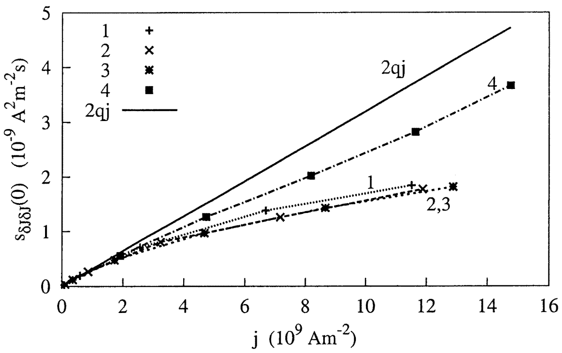

Fig. 5. Low-field spectral density of current fluctuations as function of the mean current density calculated at different frequencies $f = 0.1$, 2, 5 and 10 THz (curves 1 to 4) for $U_0 = 0.7$ V and increasing values of $U_1 = 0.2$, 0.25, 0.3, 0.35 and 0.4 V (points from left to right at each frequency).

ponent on the carrier motion in the depletion region. Accordingly, the mean current also sharply decreases.

The results seen above for the generated harmonics and the intrinsic noise of the SBD are obtained by treating separately the regular and the noise component of the current response to the applied voltage. An alternative approach [10], [11], which does not imply such a separation and calculates the spectral densities through the direct finite Fourier transform of the fluctuating current $J(t)$, has proven the complete additivity of the regular and noise components of $J(t)$ in determining the spectral density of current response of SBD

$$S_{JJ}(\nu) = \overline{s}_{\delta J \delta J}(\nu_m) A + 2T \left| j_m \right|^2 A^2 \delta_{\nu \nu_m} \tag{1}$$

where $\nu_m = mf$ and $|j_m|$ are respectively the frequency and amplitude of the m-th harmonic $(m = 1, 2, 3, \ldots)$ of the total current response $J(t)$ to the voltage applied at frequency f, A is the SBD cross-sectional area, $\delta_{\nu \nu_m}$ is the Kroneker delta symbol, and T is the time interval used to perform the finite Fourier transform, which is usually taken as a large integer number of the applied signal period [10], [11]. Such a representation of $S_{JJ}(\nu)$ allows one [10], [11] to express the signal-to-noise ratio in terms of the threshold bandwidth

$$\Delta \nu_{th} = \frac{2A|j_m|^2}{\overline{s}_{\delta J \delta J}(\nu_m)} \tag{2}$$

in which the net intensity of the current noise is set equal to the intensity of the m-th current harmonic, and thus harmonic extraction from the noise level becomes impossible. From (1) one can also obtain a somewhat different representation of the noise-to-signal ratio as

$$Q_m \equiv \frac{f}{\Delta \nu_{th}} = \frac{\overline{s}_{\delta J \delta J}(\nu_m) f}{2A|j_m|^2} \tag{3}$$

which gives the ratio between the noise power and the power of the generated m-th harmonic assuming that the bandwidth used for harmonic extraction takes the maximum possible value $\Delta \nu = f$. As follows from (2) and (3), a decrease of the cross-sectional area deteriorates the conditions of harmonic extraction from the noise level.

By using the harmonic and noise intensities calculated here (see Figs. 2 and 3, respectively) and the value $A = 7.1 \times 10^{-14}$ m^2 from the experiments of [5], the threshold bandwidth for the second and third harmonic extraction in the subterahertz region is of about 5–10 $\times 10^2$ THz with Q of about 10^{-4}–10^{-3}. When comparing these values with analog results obtained in bulk materials [10], [11], we conclude that heavily doped GaAs SBDs exhibit conditions for frequency mixing and harmonics extraction which are much better than those of bulk materials.

In conclusion, we have carried out Monte Carlo simulations of heavily doped nanometric SBD operating under cyclostationary conditions. We have found that i) the main mechanism responsible for the nonlinearity of the current response in the frequency range 0.2–5 THz is the varactor capacitance of the SBD; ii) under barrier-limited transport (when the maximum applied voltage $U_0 + U_1 < U_b$), the intrinsic noise is the full shot noise described by the universal $2q\overline{J}$ law; iii) at $U_0 + U_1 \geq U_b$ the intrinsic noise is increasingly suppressed from the full shot noise value at increasing values of the mean current density flowing through the device.

REFERENCES

[1] A. Rydberg, B. N. Lyons, and S. U. Lidholm, "On the development of a high efficiency 750 GHz frequency tripler for THz heterodyne systems," *IEEE Trans. Microwave Theory Tech.*, vol. 40, pp. 827–830, May 1992.

[2] A. Jelenski, A. Grub, V. Krozer, and H. L. Hartnagel, "New approach to the design and the fabrication of THz Schottky barrier diodes," *IEEE Trans. Microwave Theory Tech.*, vol. 41, pp. 549–556, Apr. 1993.

[3] T. W. Crowe, J. L. Hesler, R. W. Weikle, and S. H. Jones, "GaAs devices and circuits for terahertz applications," *Infr. Phys. Technol.*, vol. 40, pp. 175–189, 1999.

[4] T. W. Crowe, "GaAs Schottky barrier mixed diodes for the frequency range 1–10 THz," *Int. J. Infr. Millim. Waves*, vol. 10, pp. 765–777, July 1989.

[5] B. L. Gelmont, D. L. Woolard, J. L. Hesler, and T. W. Crowe, "A degenerately-doped GaAs Schottky diode model applicable for terahertz frequency regime operation," *IEEE Trans. Electron Devices*, vol. 45, pp. 2521–2527, Dec. 1998.

[6] T. Gonzalez, D. Pardo, L. Reggiani, and L. Varani, "The microscopic analysis of electronic noise in GaAs Schottky barrier diodes," *J. Appl. Phys.*, vol. 82, pp. 2349–2358, 1997.

[7] E. Starikov, P. Shiktorov, V. Gružinskis, J. P. Nougier, J. C. Vaissiere, L. Varani, and L. Reggiani, "Monte Carlo calculation of noise and small-signal impedance spectra in submicrometer GaAs n^+nn^+ diodes," *J. Appl. Phys.*, vol. 79, pp. 242–252, 1996.

[8] K. Brennan and K. Hess, "High field transport in GaAs, InP and InAs," *Solid-State Electron.*, vol. 27, pp. 347–357, 1984.

[9] M. V. Fischetti and S. E. Laux, "Monte Carlo analysis of electron transport in small semiconductor devices including band-structure and space-charge effects," *Phys. Rev. B*, vol. 38, pp. 9721–9745, Nov. 1988.

[10] P. Shiktorov, E. Starikov, V. Gružinskis, L. Reggiani, L. Varani, and J. C. Vaissière, "Monte Carlo calculation of electronic noise under high-order harmonic generation," *Appl. Phys. Lett.*, vol. 80, pp. 4759–4761, June 2002.

[11] P. Shiktorov, E. Starikov, V. Gruzinskis, L. Reggiani, L. Varani, J. C. Vaissière, T. González, and S. Pérez, "Monte Carlo simulation of threshold bandwith for high order harmonics extraction," *IEEE Trans. Electron Devices*, vol. 30, pp. 1171–1178, May, 2003.

[12] M. Trippe, G. Bosman, and A. Van der Ziel, "Transit-time effects in the noise of Schottky-barrier diodes," *IEEE Trans. Microwave Theory Tech.*, vol. MTT-34, pp. 1183–1192, Nov. 1986.